

Exponential band tails in polycrystalline semiconductor films

J. Werner

Max-Planck-Institut für Festkörperforschung, D-7000 Stuttgart 80,
Federal Republic of Germany

M. Peisl

Siemens AG, Zentrale Forschung und Entwicklung, D-8000 München 83,
Federal Republic of Germany

(Received 14 January 1985)

We present measurements of the energy distribution of interface states at grain boundary areas in fine-grained silicon films. A dc method as well as ac-admittance spectroscopy reveals exponentially decaying band tails in the two-dimensional density of states within the band gap. The experimental results are in agreement with a model of potential fluctuations. This model explains the extrapolated band-edge values of the density of states as well as the ratio of the slopes of conduction- and valence-band tails.

The electronic behavior of polycrystalline semiconductors is dominated by their inherent grain boundary areas where charge in interface states creates a potential barrier. Models of current transport^{1,2} across boundaries as well as of capacitance transients³ were used to attribute this charge to monoenergetic centers within the band gap, whereas experiments on bicrystals,⁴⁻⁶ as well as on films,^{7,8} revealed continuous energy distributions. Nearly all papers in the field of polycrystalline semiconductors so far assumed a spatially homogeneous barrier. It has, however, been shown⁶ that even grain boundaries in high-quality, specifically prepared bicrystals exhibit potential fluctuations due to the spatial distribution of grain boundary defects.

This Rapid Communication shows that the electronic properties of polycrystalline silicon films are primarily determined by such potential fluctuations. We find the density of states (DOS) at the grain boundaries to be dominated by exponentially decaying band tails, that are caused by localization of carriers within the wells and hills of potential fluctuations. Measurements and identification of deep exponential band tails in a two-dimensional system are reported here for the first time.

The polycrystalline silicon of 500 nm thickness is deposited by chemical vapor deposition at 625 °C. Doping up to $1 \times 10^{18} \text{ cm}^{-3}$ is performed by implantation of arsenic or boron. The grains grow columnarly with an average lateral size of 100 nm. Samples for dc characterization are deposited on oxidized silicon wafers and are provided with contact stripes for four-point measurements. ac admittance is measured at $300 \times 300 \mu\text{m}^2$ metal (aluminum)-oxide-polycrystalline silicon-silicon (MOPS) capacitors. They are fabricated by deposition of 300-nm-thick oxide onto polycrystalline silicon, which in turn is deposited on 0.5-Ω cm unoxidized wafers.

The first method we apply for DOS measurements, the *doping method*, is based on the temperature dependence of the films dc conductivity. Various models for the dc-current transport by majority carriers across grain boundaries have been proposed: thermionic emission over the potential barriers,¹ thermionic field emission,² and drift and diffusion processes.^{9,10} We describe the boundaries within the films with the help of a band diagram as shown in Fig. 1 and use a common feature of these current models. In all

of these descriptions the dc conductivity σ can be written as

$$\sigma = A(T) \exp[-e(\zeta + \phi)/kT] \quad (1)$$

Here $e\zeta$ gives the Fermi level in the grains, $e\phi$ the boundary barrier, and kT/e the thermal voltage. The prefactor $A(T)$ differs for theories of the thermionic type^{1,2} and the diffusion type.^{9,10} In the first case it contains the Richardson constant of majority carriers, in the latter one their mobility. We interpret $e\phi$ in Eq. (1) as an average barrier because the potentials at the grain boundaries fluctuate.⁶ These fluctuations may be caused by spatial variations of the band gap due to strain ("elastic fluctuations") or due to a statistical spatial distribution of charged deep centers ("electrostatic fluctuations").

The dc conductivity of our films is thermally activated

$$\sigma = \sigma_\infty \exp(-E_a/kT) \quad (2)$$

where E_a gives the activation energy, and σ_∞ is the σ value at $1/T = 0$. From Eqs. (1) and (2)

$$E_a = e\zeta(T) + e\phi(T) + kT \ln[\sigma_\infty/A(T)] \quad (3)$$

Figure 1 shows that the first two terms in Eq. (3) give the Fermi level at the interface $E_F = e\zeta + e\phi$, which controls the

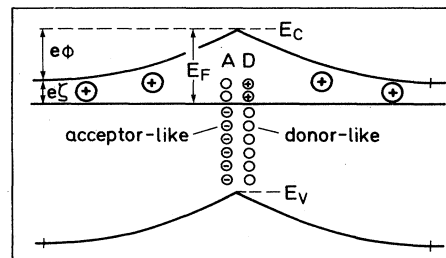


FIG. 1. One-dimensional band diagram of a charged grain boundary in *n*-type silicon. The net-negative interface charge of donor-like and acceptor-like interface states is compensated by the positive donors within the space-charge region. The measured energy distribution of the interface states is shown in Fig. 2.

occupation of the traps. From Eq. (3) it then follows

$$E_a = E_F(T=0). \quad (4)$$

The activation energy E_a gives a measure for E_F when extrapolated to zero temperature. This holds as far as $A(T)$ varies as T^α , where α is a constant, being $\alpha=1$ for thermionic emission.⁶ In the diffusion limit⁹ $A(T)$ depends linearly on mobility, which for electrons in silicon varies as $T^{-2.5}$ and for holes as $T^{-2.7}$.¹¹ We assume E_F to be independent of temperature due to pinning by the high DOS. Then Eq. (4) holds also for 250–400 K, where we measure the thermally activated behavior of σ .

When E_F is known from E_a , the barrier $e\phi$ is calculated by $e\phi = E_a - e\zeta$, where $e\zeta$ is known from Hall effect. The trapped areal boundary charge eQ is given by $eQ = (8\epsilon\epsilon_0 Ne\phi)^{1/2}$,¹ where $\epsilon\epsilon_0$ is the permittivity and N the grain doping. Experimentally we find a dependence of Q upon the doping of the films, because the changes of $N, e\zeta$ shift E_F through the DOS at the interface. Conversely, we calculate the areal density of states N_{ss} , by the derivative of Q with respect to E_F , which both depend on doping N :

$$N_{ss}(E_F) = \frac{dQ}{dE_F} = \frac{dQ}{dN} \bigg/ \frac{dE_F}{dN}. \quad (5)$$

Results of this doping method are represented by the triangles of Fig. 2. The full circles give results of films which are treated in atomic hydrogen at 400 K. This process reduces the DOS.

For our second method, *admittance spectroscopy*, we analyze the ac admittance of the MOPS capacitors of the left inset in Fig. 3. Owing to the columnar grain growth of the polycrystalline silicon the boundary areas are nearly all perpendicular to the MOS interface. The thickness δ of the grain boundary layers typically is of the order of $\delta \approx 1$ nm. We keep the analysis simple and one-dimensional and treat the boundary traps as if homogeneously distributed over the whole polycrystalline silicon layer, i.e., as bulk traps, and we

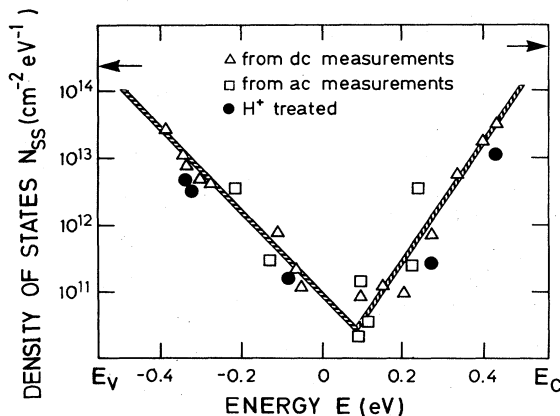


FIG. 2. Density of states (DOS) within the forbidden gap of polycrystalline silicon. Energy zero point at midgap. Data for $E < 0$ arise from p -type samples, for $E > 0$ from n -type samples. Triangles are obtained by doping method, squares by admittance spectroscopy. The lines represent least-square fits of Eq. (7) to triangles and squares. The two arrows at the band edges indicate the theoretical values for a two-dimensional free-carrier gas. Results for hydrogen-treated films are obtained by doping method.

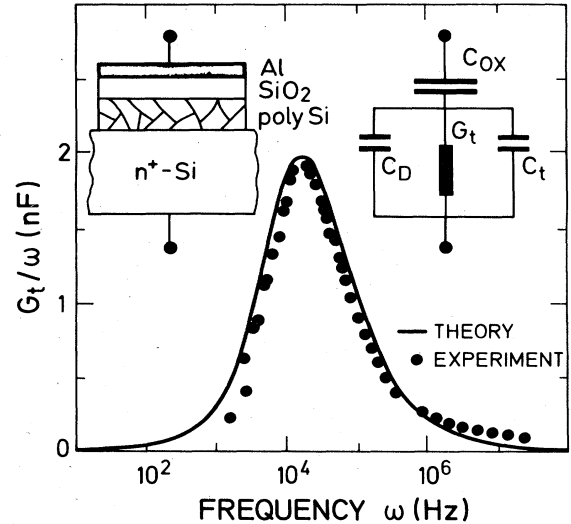


FIG. 3. Frequency dependence of interface-state conductance G_t/ω . The heavy curve arises from Eq. (6) after the determination of N^* and τ from the maximum of the measured curve. Insets show MOPS capacitor and equivalent circuit used. The capacitances of the oxide and the space-charge region are termed as C_{ox} and C_D , respectively.

finally correct for the ratio of the grain diameter to a typical boundary width, 100/1 nm. The admittance of MOS capacitors with monoenergetic bulk traps was calculated by Conti, Fischetti, and Gastaldi.¹² We extend their analysis to a continuum of energy states and write for the areal interface states admittance $Y_t = G_t + \omega C_t$ in terms of conductance G_t and capacitance C_t , in n -type polycrystalline silicon

$$Y_t = \frac{e^2 N^* x_D}{\tau} \left[\frac{1}{2} \ln(1 + \omega^2 \tau^2) + i \arctan(\omega \tau) \right]. \quad (6)$$

Here ω is the frequency $i = (-1)^{1/2}$, and $\tau^{-1} = v_n \sigma_n n$, where σ_n is the capture cross section for electrons, v_n their thermal velocity, and n their concentration at the grain boundary. The quantity N^* gives the three-dimensional DOS of bulk traps. The term in square brackets arises from an integration over energy,¹³ whereas the term $x_D/2$ arises from the integration over the depletion layer of width x_D and capacitance C_D .¹²

We calculate conductance G_t and capacitance C_t from the measured admittance with the help of the equivalent circuit of the right inset in Fig. 3. The capacitance C_{ox} is known from oxide thickness, whereas C_D, x_D are obtained from Poisson's equation.¹² The DOS of bulk traps N^* , is found from a plot of G_t/ω versus frequency as shown in Fig. 3. The maximum of the curve occurs at $\omega\tau = 1.98$ with a value of $0.2 e^2 N^* x_D$. We measure four MOPS capacitors connected in parallel and therefore get $N^* = 3.3 \times 10^{17}/\text{cm}^3 \text{ eV}$ with $x_D = 500$ nm. This corresponds to a three-dimensional DOS of $N_t = 3.3 \times 10^{19}/\text{cm}^3 \text{ eV}$ at the grain boundaries and a two-dimensional value of $N_{ss}(E_F) = N_t \delta = 3.3 \times 10^{12}/\text{cm}^2 \text{ eV}$. The capture cross sections found are 10^{-14} cm^2 for electrons and holes. Results of this second method are characterized by the squares in Fig. 2. The different squares arise from samples with different doping levels, i.e., different positions of the Fermi level E_F at the grain boundary.

We interpret the exponential behavior in Fig. 2 as band tailing: Fluctuations in the spatial distribution of grain boundary defects inevitably lead to potential fluctuations. The hills and wells of these fluctuations then give rise to localized tail states. We compare our results with a recently discussed model,¹⁴ which gives the DOS of band tails in a two-dimensional system at an energy distance ΔE from a band edge as

$$N_{ss}(E) = N_0 \exp(-\Delta E/E_0) \quad (7)$$

Here we neglect any influence of short-wavelength fluctuations on localization energy for carriers of mass m and take $E_0 = W^2 L^2 m / 2\pi^2 \hbar^2$ for the random potential of variance W^2 and correlation length L , which is expected to be of atomic size.¹⁴ The quantity ΔE in Eq. (7) is taken as $\Delta E = E_C - E$ and $\Delta E = |E_V| - |E|$ for positive and negative energies E from midgap, respectively.

We test this quantum-well model and fit Eq. (7) to the triangles and squares of Fig. 2. The results are represented by the two lines. The preexponential N_0 and the E_0 values of Eq. (7) give the extrapolated N_{ss} value at the band edges and the reciprocal value of the slope in Fig. 2. From the fit we find $N_0^C = 4.5 \times 10^{14}/\text{cm}^2 \text{eV}$, $E_0^C = 49 \text{ meV}$ for the conduction-band tail, whereas for the valence-band tail $N_0^V = 2.4 \times 10^{14}/\text{cm}^2 \text{eV}$, $E_0^V = 69 \text{ meV}$ are found. These extrapolated N_0 values should be comparable to the theoretical values for a two-dimensional (2D) gas of *delocalized* electrons and holes at the edges of the conduction and valence

bands. These two values^{15,16} of $N_{2D}^C = 4.2 \times 10^{14}/\text{cm}^2 \text{eV}$ for electrons and $N_{2D}^V = 2.3 \times 10^{14}/\text{cm}^2 \text{eV}$ for holes are indicated by the two arrows in Fig. 2 and they are close to the experimentally extrapolated DOS values. The model explains also the asymmetry in Fig. 2. The DOS masses of 0.55 and 0.33 for holes and electrons predict a theoretical value¹⁷ of

$$\gamma = E_0^V / E_0^C = 0.55/0.33 = 1.7$$

for the ratio of the slopes. From Fig. 2 we find $\gamma = E_0^V / E_0^C = 1.4$. From the E_0 values we, moreover, estimate L . The square root of variance W^2 will not exceed about half of the band-gap energy because deeper wells and higher hills in the distribution of potentials would be hindered by free-carrier screening. We then obtain a lower limit of $L \geq 1 \text{ \AA}$ for the correlation length L , which indeed is of atomic size, as expected.

In conclusion we have shown that the DOS at grain boundaries in silicon films is dominated by exponential band tails. We propose that these tails arise from localized states in quantum wells, which are caused by the statistical distribution of interface defects. The experimental results are in good agreement with this model.

The authors gratefully acknowledge numerous valuable discussions with H. J. Queisser, U. Ekenberg, and A. W. Wieder. We thank Siemens Research Laboratories for supplying us with samples.

¹J. Y. W. Seto, J. Appl. Phys. **46**, 5247 (1975).

²N. C. C. Lu, L. Gerzberg, C. Y. Lu, and J. D. Meindl, IEEE Trans. Electron. Devices **ED-30**, 137 (1983).

³A. Broniatowski and J.-C. Bourgoin, Phys. Rev. Lett. **48**, 424 (1982).

⁴C. H. Seager and G. E. Pike, Appl. Phys. Lett. **35**, 709 (1979).

⁵J. Werner, W. Jantsch, and H. J. Queisser, Solid State Commun. **42**, 415 (1982).

⁶J. Werner, in *Polycrystalline Semiconductors—Physical Properties and Applications*, edited by G. Harbeke, Springer Series in Solid State Sciences, Vol. 57 (Springer, Berlin, 1985), p. 95.

⁷S. Hirae, M. Hirose, and Y. Osaka, J. Appl. Phys. **51**, 1043 (1980).

⁸H. C. de Graaff, M. Huybers, and J. G. de Groot, Solid-State Electron. **25**, 67 (1982).

⁹W. E. Taylor, N. H. Odell, and H. Y. Fan, Phys. Rev. **88**, 867 (1952).

¹⁰M. Peisl and A. W. Wieder, IEEE Trans. Electron. Devices **ED-**

30, 1792 (1983).

¹¹K. Seeger, *Semiconductor Physics* (Springer, Wien, 1973), p. 135.

¹²M. Conti, M. V. Fischetti, and R. Gastaldi, Solid-State Electron. **25**, 5 (1982).

¹³E. H. Nicollian and A. Goetzberger, Bell Syst. Tech. J. **46**, 1055 (1967).

¹⁴C. M. Soukoulis, M. H. Cohen, and E. N. Economou, Phys. Rev. Lett. **53**, 616 (1984).

¹⁵T. Ando, A. B. Fowler, and F. Stern, Rev. Mod. Phys. **54**, 437 (1982), Eq. (2.3).

¹⁶For hole calculated with $m = 0.55$. For electrons we average over the DOS values for the (001), (011), (111) surfaces.

¹⁷Here we take the same $W^2 L$ for the two tail branches. An eventual m dependence of these two quantities could be estimated when Thomas-Fermi screening is applicable. However, the present case is more complicated since the grain boundaries are depleted from free carriers but contain localized states.